Advanced Optical Technologies

TYPE Original Research
PUBLISHED 06 January 2026
DOI 10.3389/aot.2025.1739755

OPEN ACCESS

EDITED BY
Rajib Biswas,
Tezpur University, India

REVIEWED BY
Wei Ren,
Xi'an University of Posts and Telecommunications, China
Ritu Agarwal,
ABES Engineering College, India

*CORRESPONDENCE
Xinning Huang,
huangxinning@yzu.edu.cn

RECEIVED 05 November 2025
REVISED 14 December 2025
ACCEPTED 16 December 2025
PUBLISHED 06 January 2026

CITATION
Huang X, Shen Y and Song D (2026) Performance analysis of a multi-format compatible all-optical data access method for satellite backbone-networks.
Adv. Opt. Technol. 14:1739755.
doi: 10.3389/aot.2025.1739755

Performance analysis of a multi-format compatible all-optical data access method for satellite backbone-networks

Xinning Huang[1]*, Yuerong Shen[1] and Daming Song[2]

[1]School of Physics Science and Technology, Yangzhou University, Yangzhou, China, [2]Aerospace Laser Technology and System Department, Wangzhijiang Innovation Center for Laser, Shanghai Institute of Optics and Fine Mechanics of CAS, Shanghai, China

Optical inter-satellite links are a promising technology for constructing satellite backbone networks, owing to their high data transmission capacity and lightweight terminals. To circumvent the data-rate bottlenecks and structural complexity associated with optical-electrical-optical conversion, all-optical signal processing is essential. This paper addresses a common challenge at the relaying nodes of satellite backbone networks: handling concurrent access requests from multiple laser links. We propose and validate an all-optical data access system based on an optical time-lens. The system demonstrates robust performance and high modulation format compatibility. It successfully processes intensity-modulated, phase-modulated, and hybrid-format inputs entirely in the optical domain. The system's reliability is further confirmed under practical conditions, including uneven wavelength spans and unequal data rates among the accessing links. It achieves bit-error rates below 10^{-7} and supports optical inter-satellite link transmission distances exceeding 4,500 km, even under hybrid modulation formats. With its simple structure and high compatibility, the proposed system offers a scalable solution for future multi-format satellite backbone networks.

KEYWORDS

all-optical signal processing, four-wave mixing, modulation format compatibility, optical inter-satellite links, space laser backbone network

1 Introduction

Satellite communication networks are now considered as an indispensable part of the space-air-ground integrated network architecture. This architecture aims to offer seamless coverage anytime and anywhere in the Beyond 5G (B5G) and 6G era. Especially for remote or sparsely populated areas such as mountainous, desert, or oceanic regions, satellite communication networks can be an effective alternative at lower economic costs for construction, management and maintenance (Meenu et al., 2024; Li et al., 2024a; Toyoshima, 2021; Mao et al., 2024; Zhou et al., 2024). Recently, the rapid expansion of cloud computing, big data, and the Internet of Things (IoT) has created relentless demand for high-bandwidth, large-capacity data transmission services. Consequently, optical inter-satellite links (ISLs) are considered as a crucial enabler for massive data transmission. They offer many advantages over existing radio frequency (RF) based ISLs. For example, optical ISLs offer higher bandwidth, enhanced security and directivity, lower transmit power, reduced terminal weight and volume. They also utilize an unlicensed spectrum, which is of

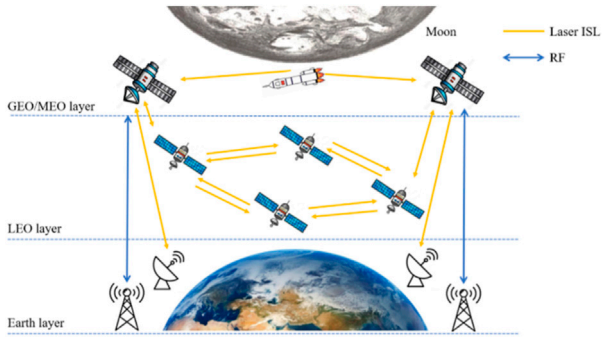

FIGURE 1
Schematic diagram of the satellite network architecture with LEO and GEO/MEO layers.

significant benefit given the escalating scarcity of the RF spectrum (Qu et al., 2022; Bhatnagar and Arti, 2013; Chan, 2024). Moreover, optical ISLs are free from atmospheric turbulence, resulting in significantly enhanced reliability and transmission distance (Hyun and Han, 2023). Consequently, low Earth orbit (LEO) satellite constellations like Kuiper, Starlink and Lightspeed, as well as geostationary orbit (GEO) satellites such as the European Data Relay System (EDRS) and the High Throughput Optical Network (HydRON) within the ScyLight program, are all actively testing or deploying optical ISLs., User data rates now exceed 10 Gb/s, with the total throughput approaching 100 Gb/s (Rieländer et al., 2022; Laguna et al., 2023).

The widely recognized architecture of optical-ISL-based satellite networks primarily comprises two layers: the GEO/medium Earth orbit (MEO) layer and the LEO layer, as illustrated in Figure 1 (Wang et al., 2024; Xia et al., 2023). LEO satellites, interconnected by optical ISLs, typically function as low-latency relay nodes with short paths. This makes them suitable for delay-sensitive services. In contrast, GEO/MEO satellites provide wider coverage. They are ideal for relaying delay-tolerant data from the LEO layer or deep space to ground stations, thereby reducing the number of hops and enhancing overall performance (Liang et al., 2024; Chaudhry et al., 2023). This architecture enables seamless communication between any space, air, or ground terminals via access to the satellite network.

Furthermore, space terminals may employ different modulation formats depending on their specific purposes and functions. This leads to a coexistence of diverse formats within the integrated networks. For instance, on-off keying (OOK) is widely used among LEO satellites due to its simplicity and maturity, as seen in DLR's OSIRIS. Pulse-position modulation (PPM) is often considered for deep-space ultra-long-distance transmission because of its superior power efficiency compared to OOK, exemplified by NASA's Deep Space Optical Communications (DSOC). Meanwhile, coherent modulation formats, such as differential phase-shift keying (DPSK) and quadrature phase-shift keying (QPSK), are preferred for inter-satellite and high-capacity data links. Their high receiver sensitivity and strong resistance to background interference make them suitable for systems like, Japan's JDRS and ESA's EDRS (Li et al., 2022; Vieira et al., 2023; Ding et al., 2022). Consequently, when multiple optical ISLs arrive at a relay satellite simultaneously, synchronous and rapid data access processing is essential. This processing must maintain high bandwidth and low latency to ensure reliable and effective optical data transmission. Therefore, relay satellites, whether in the LEO or GEO/MEO layer, must be compatible with multiple modulation formats to accommodate the diversity of existing and future space terminals. They must also be capable of concurrently handling multiple access optical ISLs with sufficient bandwidth to meet the ever-growing data capacity demands.

To address these current and anticipated challenges, optical signal processing (OSP) technologies present simple and versatile solutions. They can effectively avoid the bandwidth bottlenecks and complex configurations commonly associated with optical-electrical-optical (OEO) conversion (Li et al., 2024b; Ji et al., 2019). Specifically, for the relay satellites described above, the optical time lens (OTL) is a particular suitable OSP method. It can optically and synchronously aggregate data from several parallel ISLs onto a single backbone link with a high aggregating data rate. This simultaneously responds to multiple access requests from various optical ISLs (Lillieholm et al., 2022). This approach can significantly reduce the size, weight, power and cost (SWaP-C) of the data access unit, which are critical factors for space terminals.

Existing research on OTL mainly focuses on ultrafast spectral analysis (Meir et al., 2025), modulation format conversion (Guan et al., 2017), ultrafast optical signal processing (Liu et al., 2025; Cheung et al., 2024) and transformation (Zhang et al., 2025). However, when implemented in satellite networks, new specifics appear that have not been considered or discussed before. These include handling mixed modulation formats and non-uniform link parameters.

In this paper, we present an OTL-based all-optical data access system for relaying optical ISLs. By selecting the four-wave mixing (FWM) nonlinear effect, we demonstrate the system's significant advantages. These include synchronous response to multi-ISL access, high processing bandwidth and format compatibility. The simplified architecture reduces the number of components, thereby lowering the SWaP-C of a satellite relay unit. The ability to handle mixed modulation formats and non-uniform link parameters concurrently is a critical requirement for practical satellite relays. Yet, this has been largely overlooked in prior OTL research. This work comprehensively addresses this gap, highlighting system innovations in multi-format and multi-ISL handling capabilities. We also discuss practical factors that can affect relaying performance, such as unequal wavelength spans and different access data rates. The constructed system exhibits excellent reliability, enhancing the flexibility of future satellite backbone networks.

2 Materials and methods

The concept of optical space-time duality establishes a correspondence between the spatial diffraction of a paraxial beam and the temporal dispersion of an optical pulse (Kolner, 1994). An OTL can be constructed by applying a temporal quadratic phase modulation (QPM), $\varphi(t) = Ct^2/2$ (where C is the linear chirp rate), to a pulse sequence. This process is analogous to the function of a spatial thin lens. When combined with a dispersive medium of length L and accumulated dispersion D (where $D = \beta_2 L$, and β_2 is

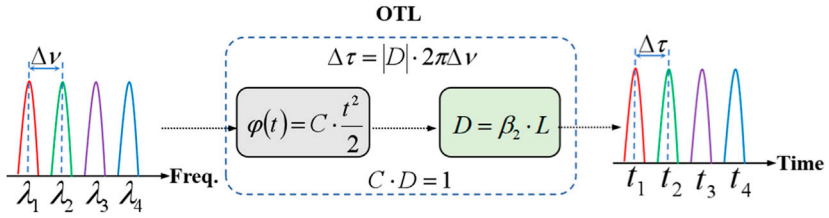

FIGURE 2
Schematic diagram of an OTL unit.

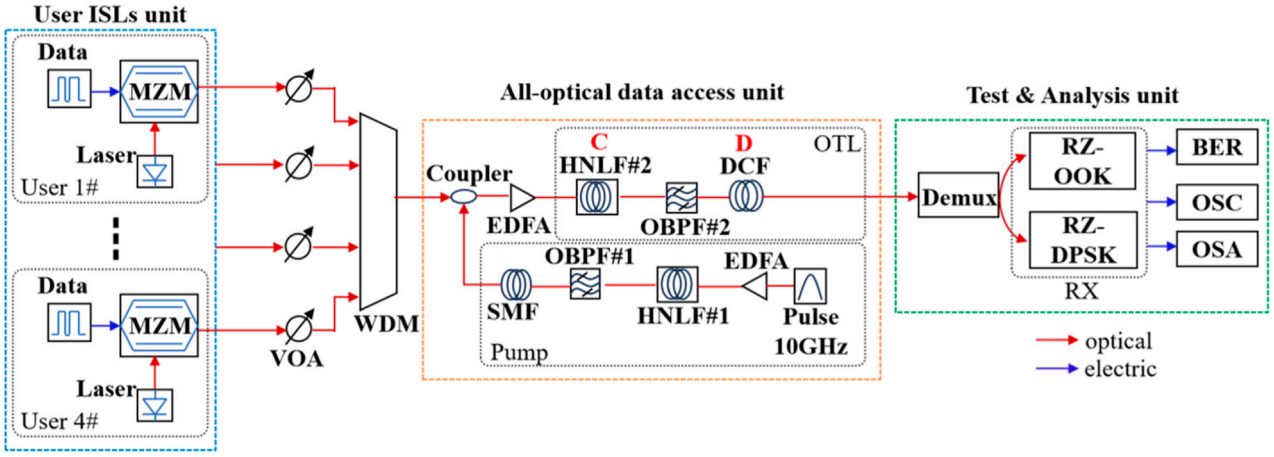

FIGURE 3
Schematic diagram of the OTL-based all-optical data access system. (MZM, Mach-Zehnder modulator; VOA, variable optical attenuator; WDM, wavelength-division multiplexer; EDFA, erbium-doped fiber amplifier; OBPF, optical bandpass filter; DCF, dispersion compensating fiber; SMF, single mode fiber; Demux, demultiplexer; RX, receiver; BER, bit error ratio tester; OSC, oscilloscope; OSA, optical spectrum analyzer).

TABLE 1 Parameters of the optical fibers used in the OTL-based system.

Parameter	SMF	DCF	HNLF#1	HNLF#2
D $(ps/nm \cdot km)$	18	−195.94	−1	−0.22
Dispersion slope $(ps/nm^2 \cdot km)$	—	—	0.006	0.0045
$\beta_2\,(ps^2/km)$	22.95	249.36	—	—
$A_{eff}\,(\mu m^2)$	72	80	10	10
$L\,(km)$	1.7346	0.0798	0.5	0.5

the second-order group-velocity dispersion coefficient), and under the condition $C \cdot D = 1$, the spectral profile of the input pulse sequence is converted into the temporal intensity profile of the output signal (Lillieholm et al., 2017; Mulvad et al., 2011). The input spectral interval $\Delta\nu$ is also mapped onto the output temporal interval $\Delta\tau$ according to the relationship $\Delta\tau = |D| \cdot 2\pi\Delta\nu$, as shown in Figure 2.

In the OTL unit, the required QPM can be achieved through other electro-optic modulation (EOM), cross-phase modulation (XPM), or FWM (Huang et al., 2023). In this work, we selected the FWM-based scheme to implement the OTL. This choice is primarily due to its superior format transparency and precision in phase manipulation, which are crucial for practical applications. In this scheme, a pump pulse (with filed E_p at frequency ω_p) is firstly chirped at a rate C/2. It is then coupled with the input ISLs (with filed E_s at ω_s) into a highly nonlinear fiber (HNLF) to stimulate the FWM effect. A newly generated idler via the FWM process (with field $E_i \propto E_p^2 \cdot E_s^*$ at $\omega_i = 2\omega_p - \omega_s$) acquires the QPM with chirp rate C from the pump pulse (Ding et al., 2022). Subsequently, propagating this idler through the dispersive medium, as described earlier, the data from all input ISLs are simultaneously converted onto the single idler wavelength, creating the relayed signal. A key advantage of this scheme is the format transparency originating from the FWM process, which imposes no restrictions on the modulation formats of the input ISLs.

Based on these principles, the diagram of the proposed all-optical data access system based on OTL for optical ISLs relaying is shown in Figure 3.

In the User ISLs unit, four optical carrier signals are used. Their wavelengths are 1,554.94 nm, 1,555.74 nm, 1,556.55 nm and 1,557.36 nm (following the ITU standard wavelength), with a spectral interval of $\Delta\nu = 100$GHz. They are independently modulated with 10 Gb/s data streams to emulate the access ISLs from different spatial platforms. By adjusting the bias voltage and driving amplitude of the MZMs, the modulation format can be set to

TABLE 2 Link budget for the ISL transmission configurations.

Link parameter	Symbol/Unit	Value	Note
Optical launch power	P_t/dBm	10	—
Free space loss	α/dB	−271.24/-291.24	4,500km/45,000 km
Antenna aperture (transmitter)	D_t/cm	12	—
Antenna gain (transmitter)	G_t/dB	107.7	$G_t = 10\,log_{10}(\frac{\pi D_t}{\lambda})^2$
Antenna aperture (receiver)	D_r/cm	12	—
Antenna gain (receiver)	G_r/dB	107.7	$G_r = 10\,log_{10}(\frac{\pi D_r}{\lambda})^2$

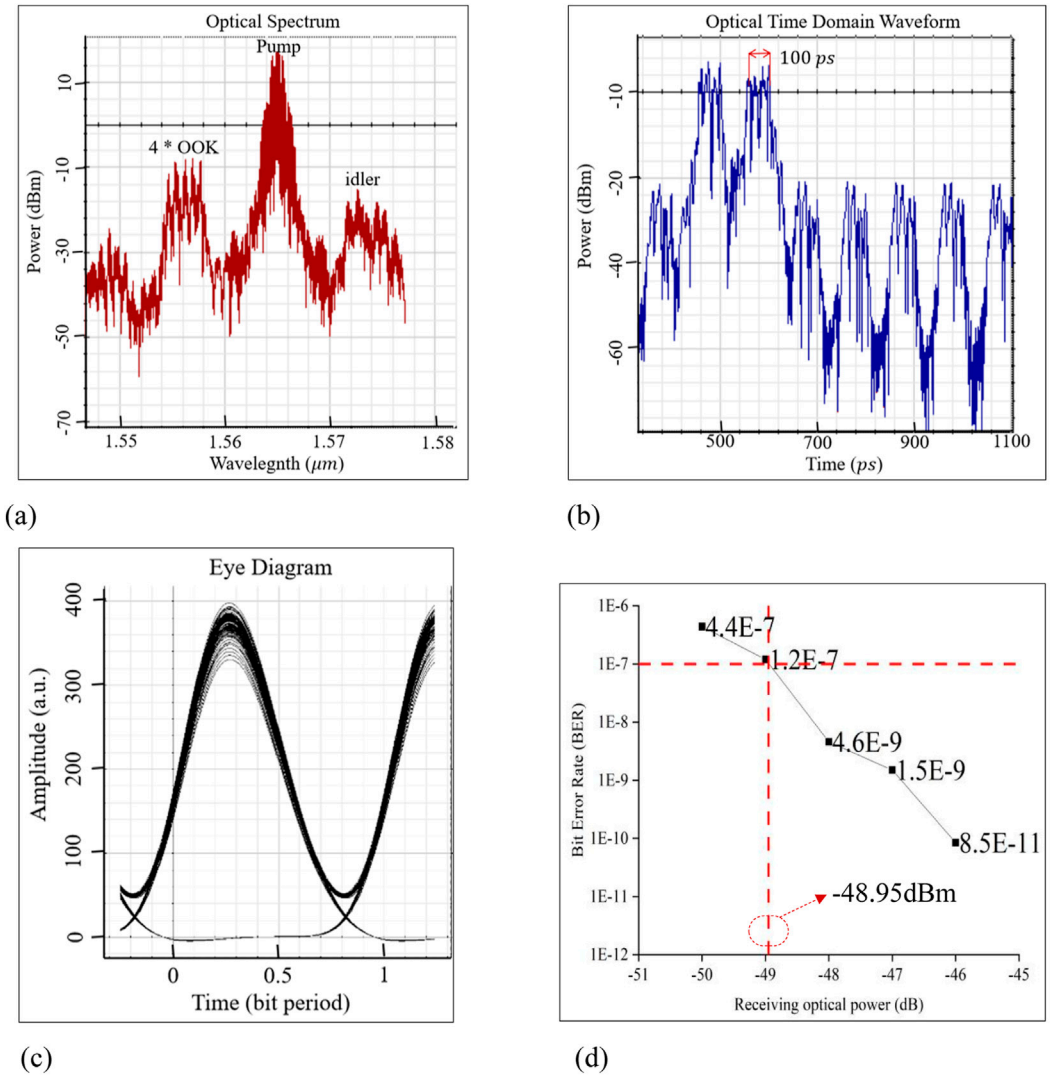

FIGURE 4
Simulation results of four identical RZ-OOK format access scenario. **(a)** Optical spectrum at the HNLF#2 output. **(b)** Optical waveform of the relayed signal. **(c)** Eye diagram of the demodulated OOK. **(d)** BER curve of the demodulated OOK.

return-to-zero OOK (RZ-OOK) or RZ-DPSK. VOAs are used to simulate the free-space loss experienced by the ISLs.

In the all-optical data access unit, a pump pulse train with 10 GHz repetition frequency and centered at 1,565.09 nm is firstly amplified. Its spectrum is broadened to 21 nm via self-phase modulation (SPM) in HNLF#1 to ensure coverage of all input signals' spectral range. After filtered with OBPF#1, the pump pulse is then linearly chirped by propagating through the SMF to

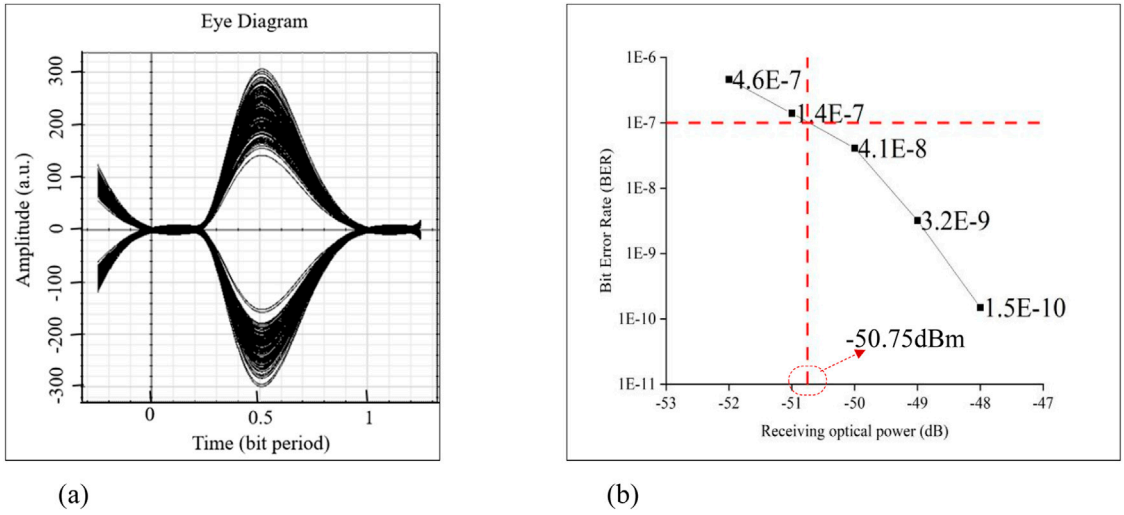

FIGURE 5
Simulation results of four identical RZ-DPSK format access scenario. **(a)** Eye diagram of the demodulated DPSK. **(b)** BER curve of the demodulated DPSK.

achieve a chirp rate of C/2 = 2GHz/ps. This specific value of C is precalculated in order to obtain a target relayed signal with data rate of 40 Gbps and temporal interval of $\Delta\tau$ = 25ps. Then this chirped pump is injected into HNLF#2 along with the combined user ISLs to stimulate the FWM process. At the output of HNLF#2, the newly generated idler (centered at 1,574.5 nm and possessing the QPM with chirp rate C = 4GHz/ps) is filtered out by OBPF#2. It is then passed through a DCF with dispersion D = 1/C to finally generate the target 40 Gb/s relayed signal. The specific parameters of the optical fibers used in this unit are listed in Table 1. These parameters values are selected to fulfill the OTL constructing requirements.

A test and analysis unit is finally constructed to evaluate the quality of the relayed signal. The high-data-rate relayed signal is demultiplexed and demodulated by corresponding receivers. Afterwards, its waveform, eye diagram, and BER are measured. The system was simulated and validated using Optisystem 15.

Furthermore, it should be noted that in practical satellite communication, the received optical power of ISLs at relay nodes can vary significantly. This is due to differing transmission distances, which may range from 4,500km to 45,000 km (Chaudhry et al., 2023; Klein et al., 2017; Qasim et al., 2024). Considering that free-space loss is the dominated power loss mechanism in space environments, this paper primarily focuses on this factor. The free-space loss α is calculated as $\alpha = 20\lg(4\pi d/\lambda)$, where d is the transmission distance and λ is the link wavelength (Xia et al., 2023). Combing with the antenna gain at the transmitter G_t and receiver G_r, the received optical power P_r is calculated by $P_r = P_t + G_t + \alpha + G_r$, with P_t the optical launch power. The detailed link budget used in our analysis is listed in Table 2, with the wavelength set to 1550 nm.

3 Results

We first evaluated the system performance under an identical format scenario by setting all four ISLs to 33% RZ-OOK. After combining with the appropriately broadened and chirped pump, they were injected into HNLF#2. During the FWM process, an idler was generated (Figure 4a), which acquired the requisite QPM from the pump and carried the data from all four ISLs. After filtering out the idler and then propagating it through the subsequent DCF, we obtained a 40 Gb/s relayed signal. Its time-domain waveform is shown in Figure 4b, where four distinct peaks are observed within each 100ps interval, corresponding to the four access ISLs. Therefore, successful access processing is confirmed.

The four time-slot tributaries were then demodulated, and one of the eye diagrams is exhibited in Figure 4c. The clean and widely open eye diagram indicates excellent signal quality. The measured BER curve is shown in Figure 4d with an average receiving sensitivity of −48.95 dBm at a BER level of 10^{-7}. This low sensitivity implies a low insertion loss of the access unit. Based on the aforementioned free-space loss calculation, it supports transmission distance of the arriving ISLs up to 6,500 km.

We then configured all four ISLs as 33% RZ-DPSK to further verify the system's compatibility with phase-modulated formats, keeping other parameters unchanged. The obtained results in Figure 5 illustrate that the system still successfully relayed the signals onto a single 40 Gb/s backbone link. One of the demodulated tributaries' eye diagram in Figure 5a remains open and clean. The measured BER curve (Figure 5b) shows a receiver sensitivity of −50.75 dBm at a BER level of 10^{-7}. This corresponds to a maximum transmission distance up to 8,000 km for the arriving ISLs. This extended range, compared to the OOK scenario, is attributed to the inherently superior receiver sensitivity of DPSK format.

Subsequently, a hybrid access scenario was investigated. This corresponds to the practical situation where ISLs from different platform may employ different modulation formats. We set two ISLs to RZ-OOK and other two to RZ-DPSK, while maintaining the same system configuration. The simulated results are presented in Figure 6. After QPM in HNLF#2 and filtering out the idler

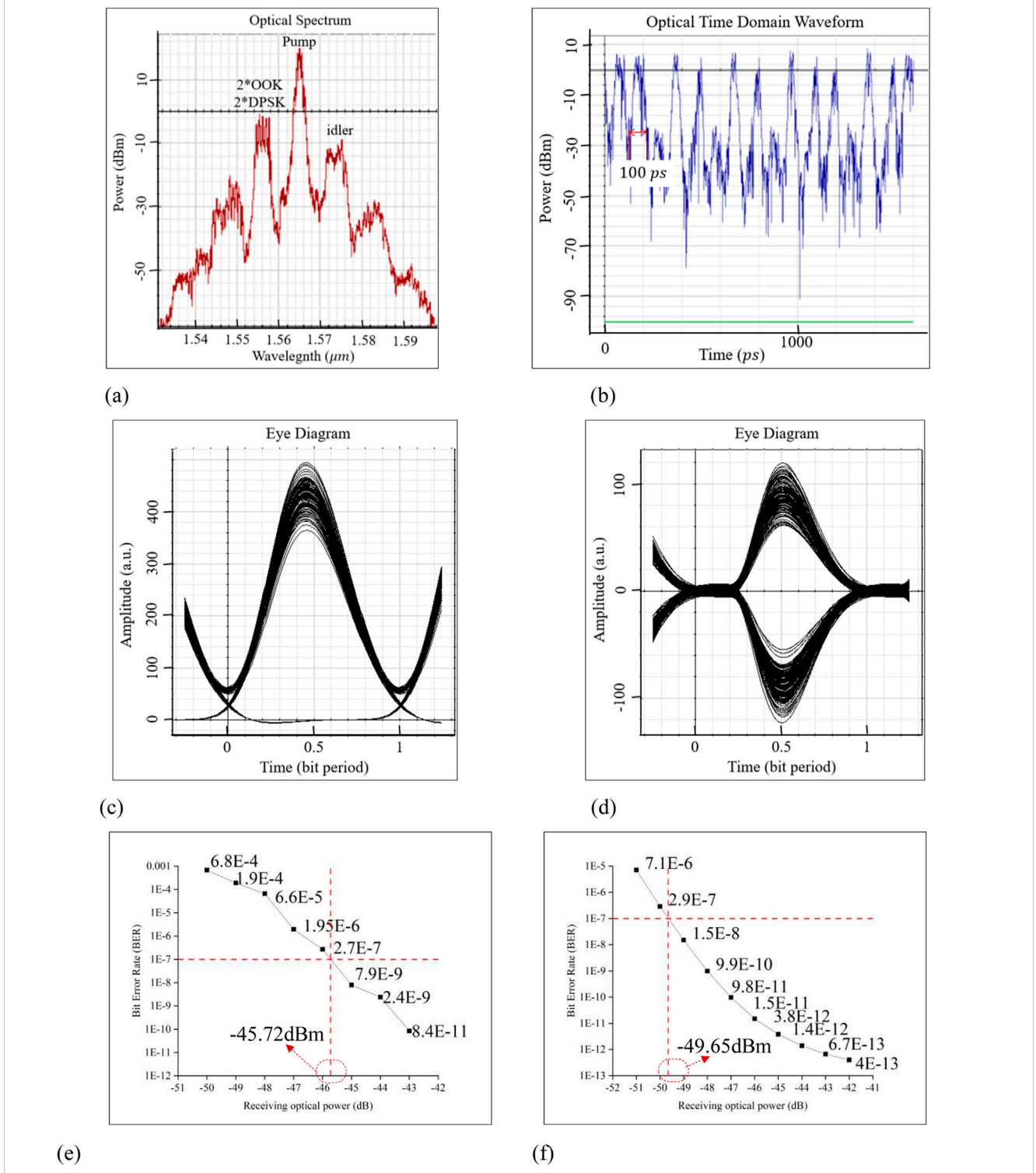

FIGURE 6
Simulation results of the hybrid access scenario. **(a)** Optical spectrum at the HNLF#2 output. **(b)** Optical waveform of relayed signal. **(c)** Eye diagram of demodulated OOK. **(d)** Eye diagram of demodulated DPSK. **(e)** BER curve of demodulated OOK (−45.72 dBm). **(f)** BER curve of demodulated DPSK (−49.65 dBm).

(Figure 6a), the generated 40 Gb/s relayed signal was transmitted through the DCF, with its optical waveform shown in Figure 6b. It is important to note that in this hybrid scenario, the relayed signal exhibits unequal pulse intervals. The reason is that OOK signals own two intensity level ("0" and "1"), whereas DPSK signals maintain a constant intensity ("1"), leading to a variable number of pulses within each 100ps interval, depending on the OOK modulation state.

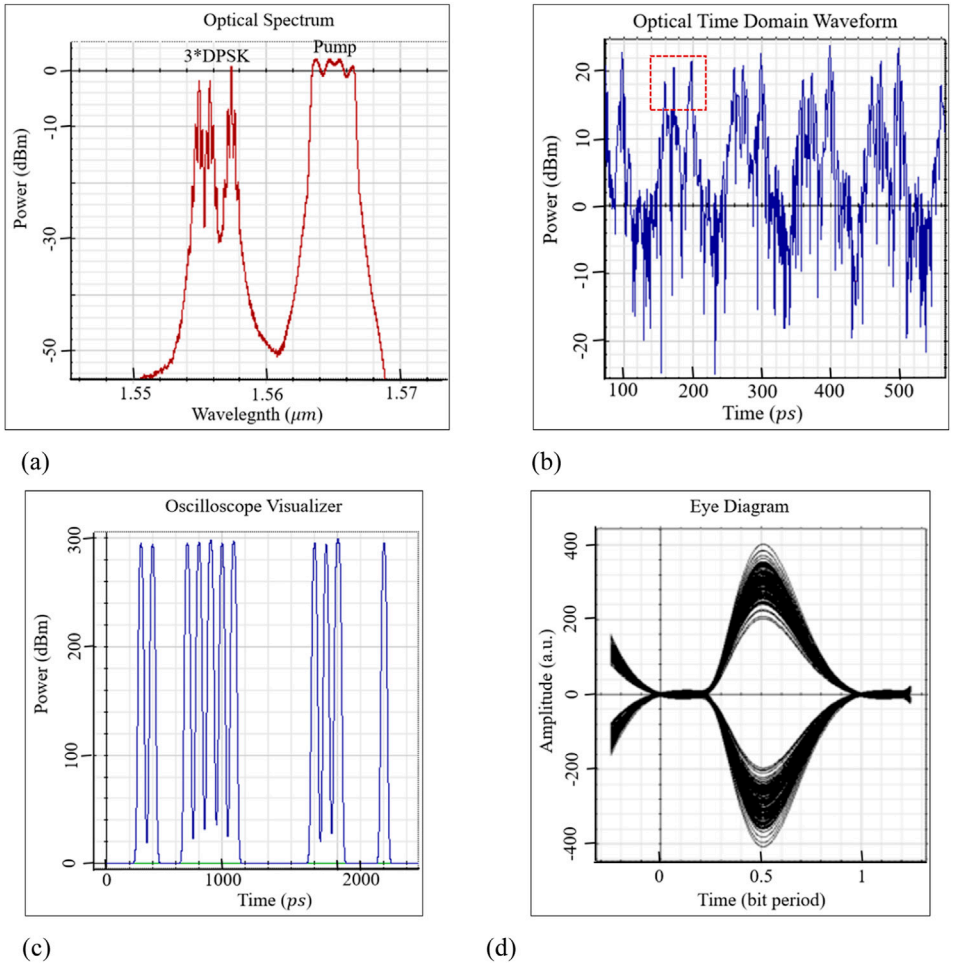

FIGURE 7
Simulation results of the uneven wavelength access scenario. **(a)** Optical spectrum at the HNLF#2 input. **(b)** Optical waveform of relayed signal. **(c)** Oscillograph of the demodulated DPSK. **(d)** Eye diagram of the demodulated DPSK.

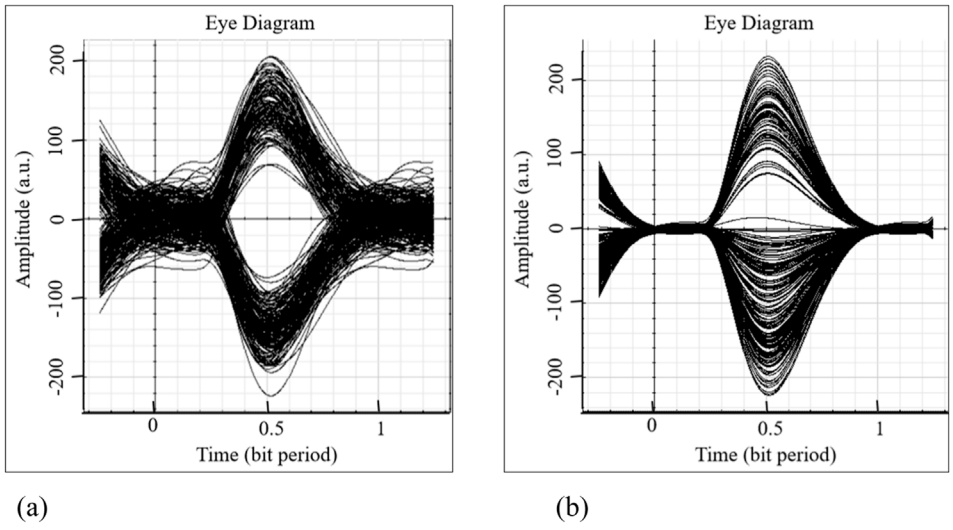

FIGURE 8
Simulation results of the demodulated signals at unequal data rates. **(a)** Eye diagram of 5 Gbps DPSK. **(b)** Eye diagram of 10 Gbps DPSK.

TABLE 3 Performance comparison of the proposed system with representative prior works.

References (Year)	Application scenarios	Modulation format	Receiver sensitivity (BER = 10^{-7})	Key features/Differences
Mulvad et al. (2011)	Fiber optical communication	OOK (single)	~-38 dBm	Single modulation, lacks considerations for space applications
Guan et al. (2014)	Fiber optical communication	DPSK (single)	~-41 dBm	
This work	Satellite (free space) optical communication	OOK & DPSK (simultaneously)	−48.95 dBm (OOK), −50.75 dBm (DPSK)	Space applications related considerations

The relayed signal was then demodulated, and the corresponding eye diagrams for the OOK and DPSK tributaries are shown in Figures 6c,d, respectively. These results confirm that the system can properly and simultaneously relay format-hybrid access ISLs, demonstrating excellent format compatibility. This feature has not been considered or discussed previously in the existing literature. It significantly broadens the system's potential application scenarios.

The measured BER curves of the demodulated OOK and DPSK tributaries are presented in Figures 6e,f. The average receiver sensitivity for OOK is −45.72 dBm at a BER level of 10^{-7}, supporting arriving ISLs with a transmission distance up to 4,500 km. For DPSK, the average receiver sensitivity is −49.65 dBm at a BER level of 10^{-7}, corresponding to a maximum transmission distance of 7,100 km for the arriving ISLs.

Although in the hybrid scenario, the access unit shows some sensitivity penalty compared to the identical-format cases, it successfully fulfills the simultaneous access requirements for links from at least 4,500 km away. This demonstrates greater flexibility and enhanced compatibility with mixed modulation formats.

We further analyzed the scenario where the access ISLs are located at unevenly spaced wavelengths. This is another practical consideration when links originate from diverse users. Here, one ISL was deactivated, leaving access signals at 1,554.94nm, 1,555.75nm, and 1,557.36nm, all modulated with identical RZ-DPSK data (Figure 7a). Other parameters remained unchanged. The optical waveform of the obtained 30 Gb/s relayed signal is shown in Figure 7b, with the temporal profile analogous to the input spectrum of the three access ISLs. The oscillograph and eye diagram of the demodulated DPSK tributaries are presented in Figures 7c,d. These results indicate that unevenly distributed wavelengths of the access ISLs do not impair the system functionality. The key difference is the deleted time slots in the relayed signal, as shown in Figure 7b. This appearance originates from the space-time duality principle of the OTL. We also found that the larger wavelength span in this case actually reduced the inter-symbol interference, leading to a better eye diagram (Figure 7d) compared to the uniform wavelength interval case (Figure 6d), and consequently, improved BER performance.

Finally, we considered the unequal data rates scenario, where accessing ISLs may operate at different data rates. We configured two ISLs at 10 Gb/s and two at 5 Gb/s, keeping other parameters unchanged. It is crucial to remember that the OTL-based system directly maps the input ISLs' spectral profile onto the relayed signal's temporal intensity profile. Consequently, the unequal data rates are not directly discernible from the relayed signal's overall waveform. Its spectrum and waveform appear similar to those in Figures 5a,b. However, while the system accurately performs the access processing function, the degraded eye diagrams of the demodulated tributaries (Figure 8) reveal deteriorated performance and a high BER floor. This performance degradation stems from the fact that the relayed signal contains all input data rates. The unequal rates cause temporal overlap and crosstalk within the relayed signal's time slots because the pulses from lower-rate links have a longer duration, severely degrading the BER performance.

4 Discussion

The escalating demand for bandwidth is accelerating the maturation of space laser communication technology. This positions optical ISLs as indispensable components of the next-generation space backbone networks. Consequently, all-optical processing at the network's relaying nodes is highly desirable. This paper presented, simulated, and validated a low-complexity, OTL-based all-optical data access system for satellite backbone networks. The system's reliability and modulation format compatibility were thoroughly examined. Simulation results confirm that the constructed system can simultaneously relay multiple ISLs with good performance. This holds true even when they employ different modulation formats or have uneven wavelength spans. These practical and vital considerations for satellite payload design have been largely overlooked in previous studies. Moreover, the system supports ISL transmission distances of at least 4,500 km under hybrid modulation formats at BER level of 10^{-7}, representing more excellent and compatible performance compared to existing solutions. More importantly, the FWM-based OTL in the proposed system is inherently format-transparent. This means the fundamental principle imposes no restriction on the modulation format, making the system compatible with other formats.

Table 3 compares the key performance metrics of our proposed OTL-based access system with those reported in representative studies on OTL (Mulvad et al., 2011; Guan et al., 2014). Our system demonstrates competitive or superior receiver sensitivity. It uniquely offers simultaneous multi-format (OOK/DPSK) and multi-ISL handling capability, which are not typically featured in the compared works.

The performance degradation observed in the unequal data rate scenario highlights a limitation of the current OTL mapping principle for handling asynchronous rate mixtures. This suggests an area for future investigation, potentially involving optical buffering or rate adaptation techniques. As the construction of global information interconnection networks accelerates, all-optical relaying will be a cornerstone technology for space laser

backbone networks. The relaying system demonstrated in this work provides valuable technical support and a scalable architectural framework for designing future space networks.

5 Conclusion

We have proposed and validated an all-optical data access system based on an optical time lens for satellite backbone networks. The system demonstrates robust performance, achieving BERs below 10^{-7} with receiver sensitivities of −48.95 dBm for OOK and −50.75 dBm for DPSK in identical-format scenarios. This supports ISL transmission distances beyond 6,500 km. Crucially, under a hybrid OOK/DPSK input, it maintains a BER below 10^{-7} for distances up to 4,500 km, confirming its strong modulation format compatibility. Its simple structure and scalability to handle non-uniform wavelength spans make it a promising candidate for future multi-format satellite communication systems. Future work will focus on extending the system to handle higher data rates, a larger number of ISLs, and other advanced formats such as QPSK or higher-order quadrature amplitude modulation (QAM). We will also investigate methods to mitigate the performance penalty in unequal data rate scenarios.

Data availability statement

The original contributions presented in the study are included in the article/supplementary material, further inquiries can be directed to the corresponding author.

Author contributions

XH: Conceptualization, Methodology, Project administration, Supervision, Writing – review and editing. YS: Formal Analysis, Data curation, Validation, Writing – original draft. DS: Data curation, Writing – original draft, Validation, Formal Analysis.

Funding

The author(s) declared that financial support was received for this work and/or its publication. This work was supported by the National Natural Science Foundation of China (Grant No. 62301476).

Acknowledgements

The authors thank the reviewers for their constructive comments and the editors for their support.

Conflict of interest

The author(s) declared that this work was conducted in the absence of any commercial or financial relationships that could be construed as a potential conflict of interest.

Generative AI statement

The author(s) declared that generative AI was not used in the creation of this manuscript.

Any alternative text (alt text) provided alongside figures in this article has been generated by Frontiers with the support of artificial intelligence and reasonable efforts have been made to ensure accuracy, including review by the authors wherever possible. If you identify any issues, please contact us.

Publisher's note

References

Bhatnagar, M. R., and Arti, M. K. (2013). Performance analysis of hybrid satellite-terrestrial FSO cooperative system. *IEEE Phot. Technol. Lett.* 25 (22), 2197–2200. doi:10.1109/lpt.2013.2282836

Chan, V. W. S. (2024). Optical Satellite Network Architecture [Invited Tutorial]. *J. Opt. Commun. Netw.* 16 (1), A53–A67. doi:10.1364/jocn.499822

Chaudhry, A. U., Lamontagne, G., and Yanikomeroglu, H. (2023). Laser intersatellite link range in free-space optical satellite networks: impact on latency. *IEEE Aerosp. Electron. Syst. Mag.* 38 (4), 4–13. doi:10.1109/maes.2023.3241142

Cheung, C., Ren, X., Lee, C. H., Kopparapu, R., Yue, Y., Chen, Z., et al. (2024). Lithium niobate chip-based ultrafast optical signal processor. *Conf. Lasers Electro-Opt. SM4L.* 5. doi:10.1364/cleo_si.2024.sm4l.5

Ding, Y., Wang, H., Ji, Y., and Zhang, Y. (2022). All-optical multi-channel aggregator for QPSK to 16QAM based on time-lens and phase reloader in elastic optical networks. *IEEE Phot. J.* 14 (6), 1–8. doi:10.1109/jphot.2022.3221796

Guan, P. (2014). "Conversion of a DWDM signal to a single nyquist channel based on a complete optical fourier transformation," in *2014 the European conference on optical communication (ECOC)* (Cannes, France).

Guan, P., Roge, K. M., Lillieholm, M., Galili, M., Hu, H., Morioka, T., et al. (2017). Time lens-based optical fourier transformation for all-optical signal processing of spectrally-efficient data. *J. Light. Technol.* 35 (4), 799–806. doi:10.1109/jlt.2016.2614186

Huang, H., Li, Y., Qin, C., Li, W., Zhao, L., Liu, C., et al. (2023). Experimental observation of the spectral self-imaging effect with a four-wave mixing time lens. *Opt. Lett.* 48 (6), 1522–1525. doi:10.1364/OL.485428

Hyun, Y.-J., and Han, S.-K. (2023). "Pulse sharpened On-Off keying optical modulation for power efficient satellite optical communication," in *2023 conference on lasers and electro-optics Europe & european quantum electronics conference (CLEO/Europe-EQEC).*

Ji, Y., Wang, H., Cui, J., Yu, M., Yang, Z., and Bai, L. (2019). All-optical signal processing technologies in flexible optical networks. Photonic netw. *Commun* 38 (1), 14–36. doi:10.1007/s11107-019-00838-y

Klein, A., Yaron, T., Preter, E., Duadi, H., and Fridman, M. (2017). Temporal depth imaging. *Optica* 4 (5), 502–506. doi:10.1364/optica.4.000502

Kolner, B. H. (1994). Space-time duality and the theory of temporal imaging. *IEEE J. Quantum Electron.* 30 (8), 1951–1963. doi:10.1109/3.301659

Laguna, V. M. F. (2023). "Optical interconnects in airbus space systems: status, vision and challenges ahead," in *British and Irish conference on optics and photonics.*

Li, R., Lin, B., Liu, Y., Dong, M., and Zhao, S. (2022). A survey on laser space network: terminals, links, and architectures. *IEEE Access* 10, 34815–34834. doi:10.1109/access.2022.3162917

Li, X., Fan, F., Yu, H., Wang, Y., Dai, X., Yang, Q., et al. (2024a). A bidirectional multi-format/rate-adjustable integrated laser communication system for satellite communication. *IEEE Phot. J.* 16 (2), 1–6. doi:10.1109/jphot.2024.3366805

Li, X., Liu, R., and Fan, F. (2024b). All-optical suppression on the impact of sun outage in laser satellite communication systems by using a nonlinear semiconductor optical amplifier. *Chin. Opt. Lett.* 22 (2), 020602. doi:10.3788/col202422.020602

Liang, J., Chaudhry, A. U., Erdogan, E., Yanikomeroglu, H., Kurt, G. K., Hu, P., et al. (2024). Free-space optical (FSO) satellite networks performance analysis: transmission power, latency, and outage probability. *IEEE Open J. Veh. Technol.* 5, 244–261. doi:10.1109/ojvt.2023.3341409

Lillieholm, M., Guan, P., Galili, M., Møller-Kristensen, M. S., Grüner-Nielsen, L., and Oxenløwe, L. K. (2017). Optimization and characterization of highly nonlinear fiber for broadband optical time lens applications. *Opt. Express* 25 (11), 12566–12580. doi:10.1364/OE.25.012566

Lillieholm, M. (2022). "64-Channel WDM transmitter based on optical fourier transformation using a portable time lens assembly," in *Optical fiber communications conference and exhibition*.

Liu, H., Xie, Q., Ma, C., Na, Q., Wang, C., Zuo, G., et al. (2025). Optical pulse processor based on achromatic time lens assisted by compound phase modulation. *Opt. Express* 33 (19), 20754–20765. doi:10.1364/OE.562119

Mao, B., Zhou, X., Liu, J., and Kato, N. (2024). Digital twin satellite networks toward 6G: motivations, challenges, and future perspectives. *IEEE Netw.* 38 (1), 54–60. doi:10.1109/mnet.2023.3332895

Meenu, R., Sharma, A., and Malhotra, R. (2024). Performance analysis of free space optical system incorporating circular polarization shift keying and mode division multiplexing. *J. Opt. Commun.* 45 (2), 347–354. doi:10.1515/joc-2021-0187

Meir, S., Duadi, H., Refaely, O., Tamir, Y., and Fridman, M. (2025). High-order autocorrelation by a Cascade time-lens. *Opt. Lett.* 50 (15), 4782–4785. doi:10.1364/OL.567318

Mulvad, H. C. H. (2011). "DWDM-to-OTDM conversion by time-domain optical fourier transformation," in *37th European conference and exposition on optical communications (ECOC)*.

Qasim, M. (2024). "Performance improvement of hybrid FSO/Fiber optic communication system under different modulation schemes," in *2023 Al-Sadiq international conference on communication and information technology (AICCIT)*.

Qu, L., Xu, G., Zeng, Z., Zhang, N., and Zhang, Q. (2022). UAV-assisted RF/FSO relay system for space-air-ground integrated network: a performance analysis. *IEEE Trans. Wirel. Commun.* 21 (8), 6211–6225. doi:10.1109/twc.2022.3147823

Rieländer, D. (2022). ESA ground infrastructure for the NASA/JPL PSYCHE deep-space optical communication demonstration. *Int. Conf. Space Opt. (ICSO)*. doi:10.1117/12.2688805

Toyoshima, M. (2021). Recent trends in space laser communications for small satellites and constellations. *J. Light. Technol.* 39 (3), 693–699. doi:10.1109/jlt.2020.3009505

Vieira, I. P., Pita, T. C., and Mello, D. A. A. (2023). Modulation and signal processing for LEO-LEO optical inter-satellite links. *IEEE Access* 11, 63598–63611. doi:10.1109/access.2023.3287501

Wang, G., Yang, F., Song, J., and Han, Z. (2024). Free space optical communication for inter-satellite link: architecture, potentials and trends. *IEEE Commun. Mag.* 62 (3), 110–116. doi:10.1109/mcom.002.2300024

Xia, Z. (2023). "Inter-satellite link channel characterization of laser communication systems," in *2023 IEEE 11th international conference on information, communication and networks (ICICN)*.

Zhang, Y., Tao, C., Luo, S., Lau, K. Y., Zheng, J., Huang, L., et al. (2025). Ultra-fast optical time-domain transformation techniques. *Nat. Rev. Methods Prim.* 5, 11. doi:10.1038/s43586-025-00381-3

Zhou, X., Weng, Y., Mao, B., Liu, J., and Kato, N. (2024). Intelligent multi-objective routing for future ultra-dense LEO satellite networks. *IEEE Wirel. Commun.* 31 (5), 102–109. doi:10.1109/mwc.010.2300353